Neurosci. Bull. March, 2021, 37(3):298–310
https://doi.org/10.1007/s12264-020-00618-z

www.neurosci.cn
www.springer.com/12264

ORIGINAL ARTICLE

FOXG1 Directly Suppresses Wnt5a During the Development of the Hippocampus

Yang Ni[1] · Bin Liu[1] · Xiaojing Wu[1] · Junhua Liu[1] · Ru Ba[1] · Chunjie Zhao[1]

Received: 10 February 2020 / Accepted: 19 July 2020 / Published online: 3 January 2021
© Shanghai Institutes for Biological Sciences, CAS 2021

Abstract The Wnt signaling pathway plays key roles in various developmental processes. Wnt5a, which activates the non-canonical pathway, has been shown to be particularly important for axon guidance and outgrowth as well as dendrite morphogenesis. However, the mechanism underlying the regulation of Wnt5a remains unclear. Here, through conditional disruption of *Foxg1* in hippocampal progenitors and postmitotic neurons achieved by crossing *Foxg1*$^{fl/fl}$ with *Emx1-Cre* and *Nex-Cre*, respectively, we found that Wnt5a rather than Wnt3a/Wnt2b was markedly upregulated. Overexpression of *Foxg1* had the opposite effects along with decreased dendritic complexity and reduced mossy fibers in the hippocampus. We further demonstrated that FOXG1 directly repressed Wnt5a by binding to its promoter and one enhancer site. These results expand our knowledge of the interaction between *Foxg1* and Wnt signaling and help elucidate the mechanisms underlying hippocampal development.

Keywords Wnt5a · *Foxg1* · hippocampus · granule cell · pyramidal neuron · dendritic arborization · mossy fiber · Wnt

✉ Chunjie Zhao
zhaocj@seu.edu.cn

[1] Key Laboratory of Developmental Genes and Human Diseases, Ministry of Education, School of Medicine, Southeast University, Nanjing 210009, China

Introduction

Members of the Wnt family are known to be crucial in numerous developmental processes, including telencephalic patterning, cell fate determination, axon guidance, and dendritic arborization, by triggering different signaling pathways [1–7]. In the developing telencephalon, Wnt members usually exhibit unique expression patterns and are involved in distinct developmental events. Disruption of Wnt3a, which is specifically expressed in the cortical hem, a signal center that plays key roles in the patterning of the telencephalon, results in the loss of the whole hippocampus, whereas forced Wnt3a expression facilitates neurogenesis, learning, and memory in the hippocampus [8–11]. In hippocampal neurons, Wnt3a is also involved in determining axonal position and outgrowth by controlling the remodeling of microtubules [12]. Wnt2b is involved in cell fate determination through activating the canonical Wnt signaling pathway [13, 14]. Wnt2b also controls the differentiation of neural progenitor cells [15, 16]. Wnt5a usually activates the non-canonical Wnt pathway and is highly conserved from *Caenorhabditis elegans* to humans [17–19]. Wnt5a is expressed in the medial pallium of the telencephalon at early developmental stages and is postnatally expressed in postmitotic neurons in the developing hippocampus [20, 21]. Previous studies have shown that Wnt5a is required for axon guidance and outgrowth [22–26]. Moreover, recently, Wnt5a was reported to be essential for dendritic branching in hippocampal neurons [21, 27]. Despite these critical roles, the upstream regulators of Wnt5a during telencephalic development remain elusive.

Foxg1, one of the Forkhead box transcription factors, has been reported to mainly act as a transcriptional repressor [28–30]. *Foxg1*-null mutants exhibit significant

expansion of the cortical hem, where multiple Wnts are enriched [31]. The expression of Wnt3a, 2b and 5a spreads to the neocortex. FOXG1 has also been reported to direct optic development through transcriptional suppression of Wnt8b [32]. Previous studies have shown that during early facial and forebrain development, the canonical Wnt/ß-catenin signaling pathway transcriptionally targets *Fgf8* signaling, which subsequently triggers *Foxg1* expression [33, 34]. Moreover, *Foxg1* is strongly reduced in the truncated medial wall neuroepithelium in Wnt3a mutants [9]. To further elucidate the mutual interaction between *Foxg1* and Wnts and considering the role of Wnt5a in the development of dendrites, we conditionally disrupted *Foxg1* in the medial pallium and postmitotic neurons of the hippocampus and found that Wnt5a was significantly upregulated accompanied by impairments in dendritic complexity and mossy fibers. Overexpression of *Foxg1* had the opposite effects. Moreover, combined with chromatin immunoprecipitation (ChIP) analysis, these results indicated that FOXG1 directly suppresses Wnt5a. These results expand our knowledge of the interaction between *Foxg1* and Wnt signaling and the mechanisms underlying the development of the hippocampus.

Materials and Methods Animals

The *Foxg1*$^{fl/fl}$ and the *CAG-loxp-stop-loxp-Foxg1-IRES-EGFP* mouse lines were generated as previously reported [35, 36]. *Emx1-Cre* mice (stock number: 005628) were purchased from the Jackson Laboratory. *NEX-Cre* mice were generated as previously described [37]. Conditional disruption of *Foxg1* was achieved by crossing *Foxg1*$^{fl/fl}$ mice with *Emx1-Cre* or *NEX-Cre* mice. For overexpression of *Foxg1* in the progenitors and postmitotic neurons, the *CAG-loxp-stop-loxp-Foxg1-IRES-EGFP* line was crossed with the *Emx1-Cre* and *NEX-Cre* lines, respectively. The day of vaginal plug detection was considered to be embryonic day 0.5 (E0.5), and the day of birth was designated postnatal day P0. All mice were bred in the animal facility at Southeast University. Gender was not considered in this study. All experiments were performed according to the approved guidelines of Southeast University.

Immunostaining and *In Situ* Hybridization

Brains were fixed by transcardial perfusion with cold 4% paraformaldehyde (PFA) in PBS, postfixed at 4°C overnight, cryoprotected in 30% sucrose, embedded in OCT, and stored at –70°C until use. The brains were cryosectioned at 16 μm on a Leica CM 3050S cryostat. Immunostaining was then performed as previously described [35]. The following antibodies were used: guinea pig anti-Calbindin (Millipore, AB1778, 1:250), rabbit anti-Calretinin (Millipore, AB5054, 1:500), rat anti-Ctip2 (Abcam, ab18465, 1:2000), rabbit anti-FOXG1 (Abcam, AB18259, 1:500), rabbit anti-Prox1 (Millipore, AB5475, 1:1000), and mouse anti-Synaptoporin (SCBT, sc376761). The secondary antibodies were: Alexa Fluor 568 goat anti-guinea-pig IgG (Molecular Probes, A11075, 1:500), Alexa Fluor 555 donkey anti-mouse IgG (Invitrogen, A31570), Alexa Fluor 546 donkey anti-rabbit IgG (Life, A10040, 1:500), Alexa Fluor 647 donkey anti-rabbit IgG (Life, A31573, 1:500), and Alexa Fluor 546 goat anti-rat IgG (Molecular Probes, A11081, 1:500). DAPI was from Sigma-Aldrich (D9564).

In situ hybridization was performed as previously described [38]. The probes were obtained by PCR amplification.

Real-Time PCR

Total RNA was isolated from the E14.5 dorsal telencephalon using the RNeasy Plus Mini Kit (Qiagen, 74104) according to the manufacturer's instructions, and each sample was reverse-transcribed into cDNA using the PrimeScriptTM RT reagent kit with gDNA Eraser (TaKaRa, RR047A). Tissue from at least three brains of each genotype were used. Quantitative real-time PCR was performed as previously described [35]. The following primers were used for the analyses: Wnt3a-F: 5′-GCAGCTGTGAAGTGAAGAC-3′ and Wnt3a-R: 5′-GGTGTTTCTCTACCACCATCTC-3′; Wnt2b-F: 5′-GCCAAAGAGAAGAGGCTTAA-3′ and Wnt2b-R: 5′-TCAGTCCGGGTGGCGTGGCG-3′; Wnt5a-F: 5′-CTCGGGTGGCGACTTCCTCTCCG-3′ and Wnt5a-R: 5′-CTATAACAACCTGGGCGAAGGAG-3′. Each sample was analyzed in triplicate reactions. The relative gene expression of the samples was normalized to the most reliable endogenous gene (glyceraldehyde 3-phosphate dehydrogenase, GAPDH).

Western Blot

The dentate gyrus (DG) was collected at P0 after hypothermic anesthesia and prepared as described previously [35]. The primary antibodies used were rabbit anti-FOXG1 (Abcam, AB18259, 1:3000) and rabbit anti-β-actin (Cell Signaling Technology, 1:5000). HRP-linked anti-rabbit IgG (Cell Signaling Technology, 7074S, 1:3000) was used as the secondary antibody.

Microscopy and Image Analysis

Sections were viewed under a confocal microscope (Olympus FV1000), and images were collected and analyzed

using FV10-ASW image analysis software. The images were optimized for size, color, and contrast using Adobe Illustrator.

Golgi Staining and Morphometric Analysis

P17 brains were stained using an FD Rapid GolgiStain kit according to the manufacturer's instructions and as previously described [39, 40]. Briefly, brains were impregnated with Golgi solution (a mixture of solutions A and B) at room temperature in the dark for 6 days, transferred to solution C for 3 days, and sectioned at 120 μm on a vibrating microtome (VT1000; Leica Microsystems). Five brains per genotype from different parents ($n > 3$) were impregnated. Images of the dendritic arbors of pyramidal neurons and granule cells were captured under Z-stack mode using an EVOS FL Auto microscope (Life Technology) with a 40× objective lens. The dendrite of each neuron was manually traced using ImageJ software (NIH). Sholl analysis in ImageJ was used to assess the dendritic complexity by examining the number of dendritic intersections per 20-μm concentric radial distance from the soma. Significant differences in dendritic complexity were determined by two-way ANOVA (genotype and circle radius as factors) in GraphPad Prism software. Values were considered significant at $P < 0.05$.

ChIP-Seq Analyses and qPCR

Chromatin immunoprecipitation sequencing (ChIP-seq) was performed using E16.5 wild-type telencephalons with an anti-FOXG1 antibody as described previously [29]. The sequencing reads were mapped to the mouse reference genome (mm9 on the UCSC genome browser). The gene sequences for Wnt5a (NC_000080.6) were obtained using NCBI. The qPCR primers spanned three FOXG1 putative binding sites: the promoter (a) and two enhancer regions (b, c): Wnt5a-a-F: 5′-AGAGAGGAGGAGCTGACAAT-3′ and Wnt5a-a-R: 5′-AATCCCTGTGCCCAAGATG-3′; Wnt5a-b-F: 5′-GCGCAGTCAATCAACAGTAAAC-3′ and Wnt5a-b-R 5′-GGCTTCTGGAGAGGAAAGAAAG-3′; Wnt5a-c-F: 5′-CTGGCTGGCTCTGGTTT-3′ and Wnt5a-c-R: 5′-TTTCTACGCCAGAGTTTAAGAATTG-3′. The fold enrichment from three independent experiments were compared using GraphPad software to determine the statistical significance. Values are expressed as the mean ± SEM.

Luciferase assay

The mouse Wnt5a-luciferase reporter (pmrt) contains nucleotides from − 1273 to + 621 relative to the transcription start site of the mouse Wnt5a gene (NC_000080.6). The Wnt5a-enhancer 1 (E1) and 2 (E2) regions contain nucleotides from + 5241 bp to + 6441 bp and + 194.2 kb to + 195.2 kb of the transcription start site, respectively. The reporter vectors were constructed by cloning pmrt or the E1 and E2 fragments into the pGL3-basic or pGL3-promoter reporter plasmids. The primer sequences were as follows: Wnt5a-prmt-F: 5′-GCGTGCTAGCCCGGGCTCGAGGGCGCAAGGAGA-CATCCC-3′ and Wnt5a-prmt-R: 5′- ACTTAGATCGCA-GATCTCGAGGGCACGGAGAGGAAGTCGC-3′; Wnt5a-E1-F: 5′- AATCGATAAGGATCCGTC-GACCTGCTGATGCTTGGGAGCTG-3′ and Wnt5a-E1-R: 5′- CTCTCAAGGGCATCGGTCGACGAAAGAAAG-GAGCAGATGTTTATTGC-3′; Wnt5a-E2-F: 5′- AATC-GATAAGGATCCGTCGACAACATCTCTTTATATAG-TAAGGCTCTAGGATG-3′ and Wnt5a-E2-R: 5′-CTCTCAAGGGCATCGGTCGACACAAGTCCAAC-CAATCAACTAAAATAA-3′. A luciferase assay was performed using Neuro2A cells. For transfections, 1×10^5 cells per well were seeded onto 24-well plates and incubated with DMEM/F12 complex medium overnight. The second day, pGL3-basic-prmt, pGL3-promoter-E1, and pGL3-promoter-E2 were added with either pCAG EN (control) or pCAG-Foxg1 (500 ng/well for each construct) together with the SV40 plasmid containing the *Renilla* luciferase gene (50 ng/well) as an internal plasmid control. The transfection medium was replaced by complete medium containing antibiotics after 6 h of transfection. The luciferase activities were assayed 48 h after transfection. The firefly luciferase readout was normalized to the respective *Renilla* luciferase readout from the same cell lysate. The fold change in response to FOXG1 activity was calculated with respect to the controls. All the values are expressed as the mean ± SEM of three biological replicates.

Results

Abnormal Expression of Wnt5a After Deletion of *Foxg1* in the Hippocampal Primordium

To gain an in-depth understanding of the regulation of Wnt5a by *Foxg1* in the developing telencephalon, we first conditionally inactivated *Foxg1* in the dorsal telencephalic progenitors from E10.5 onwards by crossing *Emx1-Cre* mice with $Foxg1^{fl/fl}$ mice (referred to as *Emx1-Cre;Foxg1* cKO). The deletion efficiency of *Foxg1* was assessed by immunostaining for FOXG1. Compared to that of the control, FOXG1 was completely undetectable in the dorsal telencephalon, including the cortical hem, where multiple Wnts are enriched (Fig. 1A, A'). The $Foxg1^{-/-}$ mice in which *Foxg1* was deleted as early as E8.5 exhibited severe

expansion of the cortical hem with the expression of Wnt5a and Wnt3a/Wnt2b, two specific markers for the cortical hem, which spread to the whole cortex [31]. We then examined the expression of the three Wnt members at E12.5 in *Emx1-Cre; Foxg1* cKO mice. As shown in Fig. 1B and 1B', there was a slight expansion of Wnt5a in the medial pallium compared to that of controls, but no differences in the expression of Wnt3a and Wnt2b (Fig. 1C–D'), consistent with our previous report [41]. At E14.5, Wnt5a was expressed not only in the cortical hem but also in the hippocampal primordium in controls (Fig. 1E). A marked upregulation was detected in the *Emx1-Cre; Foxg1* cKO mice (Fig. 1E'). Similarly, there were no changes in Wnt3a and Wnt2b (Fig. 1F–G'). Moreover, qPCR analysis revealed that Wnt3a and Wnt2b were expressed at comparable levels in control and the *Emx1-Cre; Foxg1* cKO mice, while Wnt5a was increased by ~50% (Fig. 1H). Upregulation of Wnt5a was also evident at E16.5 in *Emx1-Cre;Foxg1* cKO mice (Fig. 1I, I'). These results suggest that FOXG1 is involved in the regulation of Wnt5a rather than Wnt3a/Wnt2b from E10.5 onwards.

Downregulation of Wnt5a After Overexpression of *Foxg1* in the Hippocampal Primordium

To confirm the regulation of Wnt5a by FOXG1, we overexpressed *Foxg1* in the dorsal telencephalon by crossing the *Emx1-Cre* line with the *CAG-loxp-stop-loxp-Foxg1-IRES-EGFP* line (referred to as *Emx1-Cre*; *CAG-Foxg1* TG) (Fig. 2A). The FOXG1 expression in the dorsal telencephalon was stronger than that of the controls (Fig. 2B and 2B'). As shown in Fig. 2B', notable ectopic expression of FOXG1 was also detected in the cortical hem

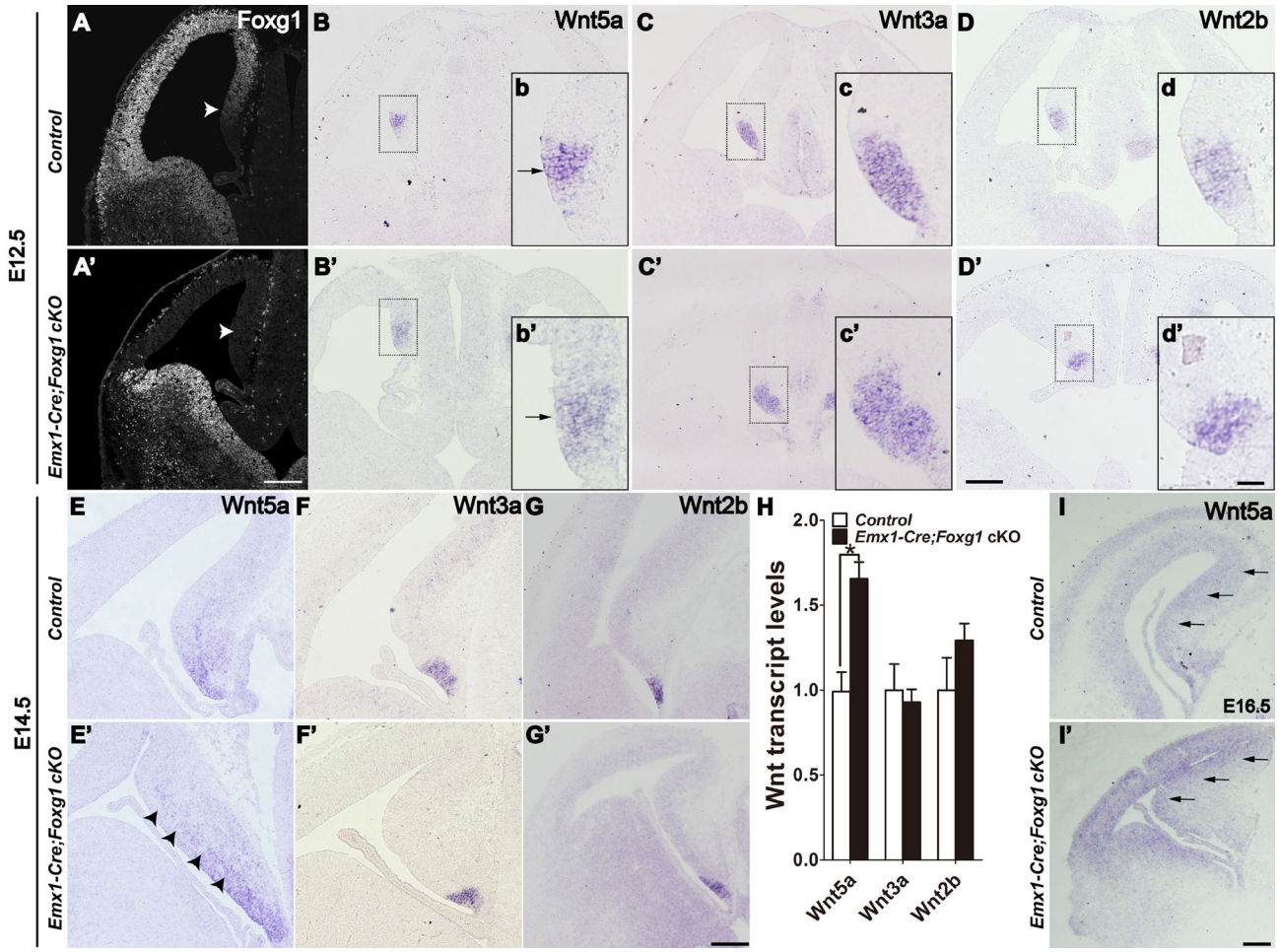

Fig. 1 Upregulation of Wnt5a after deletion of *Foxg1* in the hippocampal primordium. **A, A'** Immunostaining showing that FOXG1 is efficiently disrupted in the dorsal telencephalon, including the hippocampal primordium (arrowhead). **B–D'** *In situ* analysis of Wnt5a, Wnt3a, and Wnt2b. b–d' Magnified views of the boxed areas in **B–D'**. **E–G'** Representative *in situ* images of Wnt5a, Wnt3a, and Wnt2b in the cortical hem at E14.5. Arrows in b, b' and arrowheads in E, E' indicate the excessive expression of Wnt5a in the medial pallium. **H** qPCR analysis of Wnt5a, Wnt3a, and Wnt2b in the telencephalon. **I, I'** *In situ* analysis of Wnt5a at E16.5. Values are expressed as the mean ± SEM, $n = 3$, $^*P < 0.05$. Scale bars, (**A–I'**) 200 μm; (**b–d'**) 50 μm.

where FOXG1 was normally absent. Interestingly, Wnt5a was clearly downregulated in the cortical hem at E12.5 and almost undetectable at E14.5 (Fig. 2C, C' and 2F, F'), while Wnt3a and Wnt2b remained unchanged in the *Emx1-Cre*;*CAG-Foxg1* TG mice (Fig. 2D–E' and 2G–H'). qPCR analysis further demonstrated the downregulation of Wnt5a in the *Emx1-Cre*;*CAG-Foxg1* TG mice with both Wnt3a and Wnt2b unaltered in either case (Fig. 2I). The reduction of Wnt5a was detected as well at E16.5 in the *Emx1-Cre*; *CAG-Foxg1* TG mice (Fig. 2J, J'). Thus, FOXG1 functions upstream of Wnt5a in the developing telencephalon.

Foxg1 Regulates Wnt5a in Postmitotic Neurons

To further determine whether Foxg1 regulates Wnt5a in postmitotic neurons, we conditionally inactivated *Foxg1* by crossing *NEX-Cre* with *Foxg1*$^{fl/fl}$ mice (referred to as *NEX-Cre; Foxg1* cKO). As expected, *Foxg1* expression was eliminated in the postmitotic neurons but remained in the

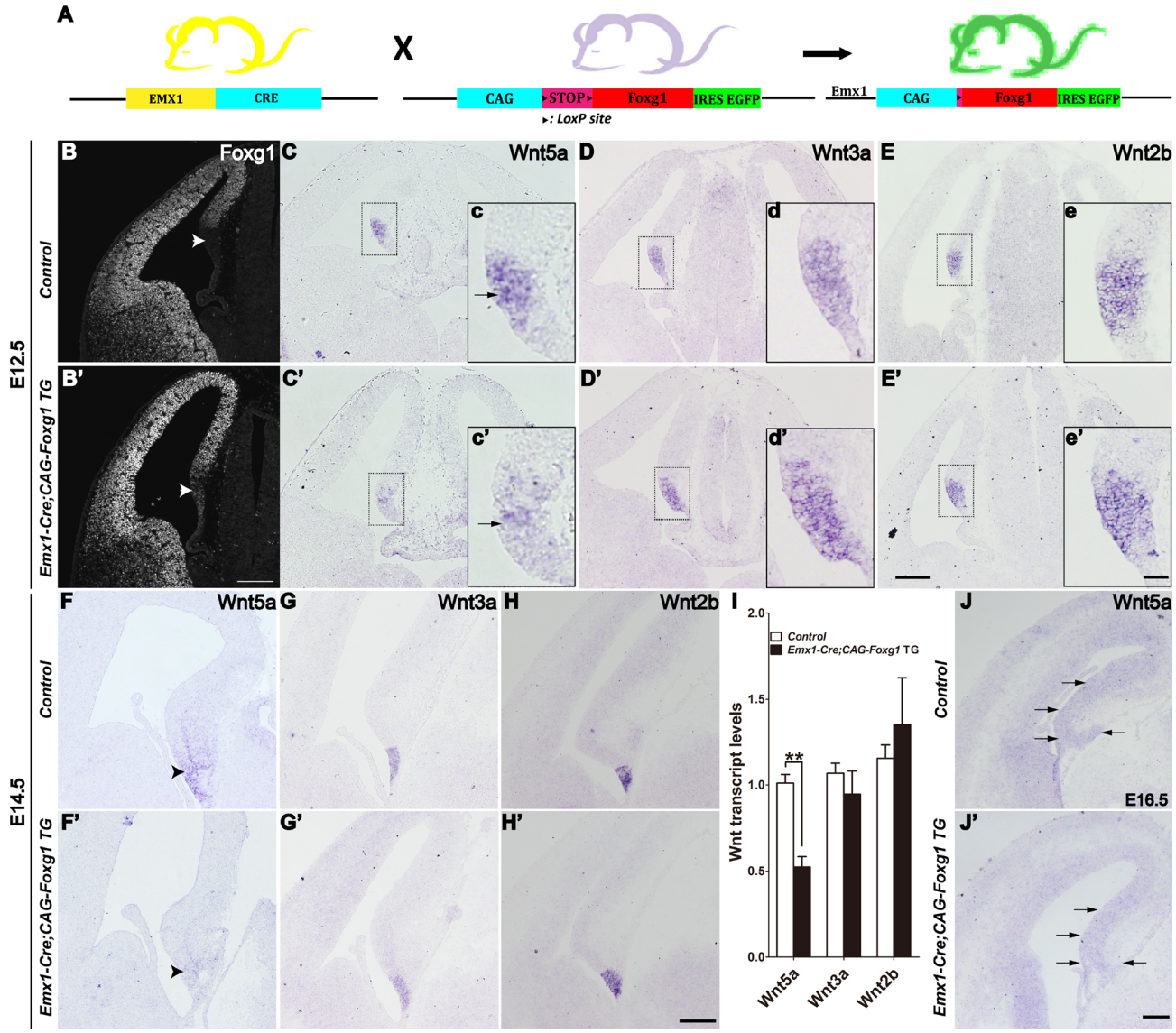

Fig. 2 Downregulation of Wnt5a after *Foxg1* overexpression in the hippocampal primordium. **A** Schematic of the strategy for overexpression of *Foxg1*. **B, B'** FOXG1 expression assessed by immunofluorescence. Arrowheads indicate ectopic expression of FOXG1 in the TG cortical hem (B'), which is normally undetectable (B). **C–E'** *In situ* hybridization of Wnt5a (**C**, **C'**), Wnt3a (**D**, **D'**), and Wnt2b (**E**, **E'**) in E12.5 controls (**C**–**E**) and *Emx1-cre;Foxg1* TG mice (**C'**–**E'**) showing downregulation of Wnt5a (arrows) and comparable levels of Wnt3a and Wnt2b. **c–e'** Magnified views of the boxed areas in (**C**–**E'**). **F–H'** *In situ* hybridization for Wnt5a (**F**, **F'**), Wnt3a (**G**, **G'**), and Wnt2b (**H**, **H'**) at E14.5. Wnt5a is almost undetectable in the hippocampal primordium (arrowheads). No changes occur in Wnt3a and Wnt2b. **I** qPCR showing a significant decrease in Wnt5a. **J, J'** *In situ* analysis of Wnt5a at E16.5. Values are expressed as the mean ± SEM, $n = 3$, $^{**}P < 0.01$. Scale bars, (**B–J'**) 200 μm; (**c–e'**) 50 μm.

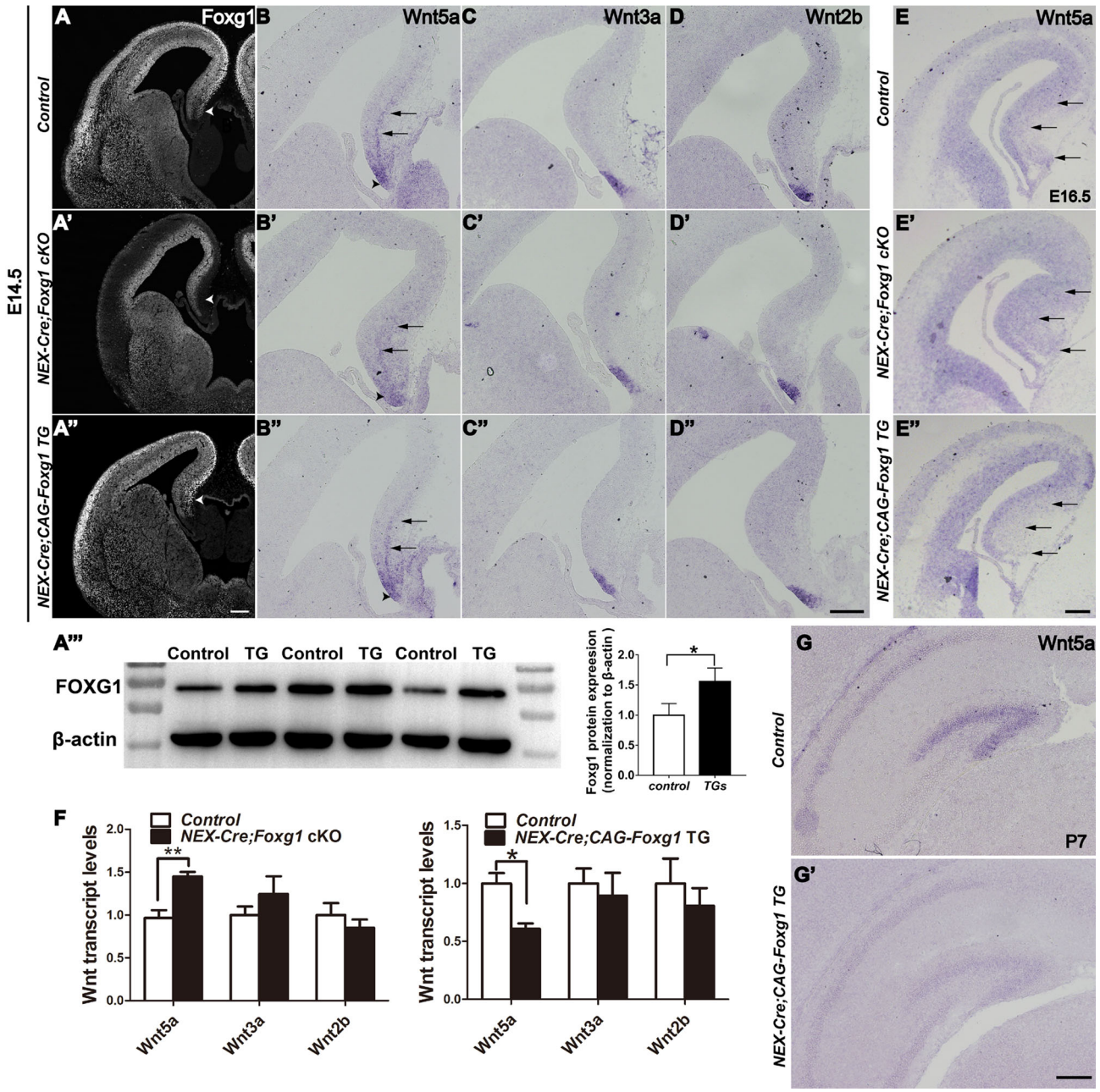

Fig. 3 Abnormal expression of Wnt5a after deletion or overexpression of *Foxg1* in postmitotic neurons. **A–A'''** Immunostaining of FOXG1 in control, *NEX-cre;Foxg1* cKO, and *NEX-cre;Foxg1* TG brains at E14.5. The arrowhead in A' indicates the loss of *Foxg1* in postmitotic neurons. **A'', A'''** Immunofluorescence and Western blot analysis of FOXG1. *Foxg1* is overexpressed in the *NEX-cre;Foxg1* TG brain. **B–D''** *In situ* hybridization for Wnt5a (**B–B**''), Wnt3a (**C–C**''), and Wnt2b (**D–D**'') in E14.5 control, *NEX-cre;Foxg1* cKO, and *NEX-cre;Foxg1* TG brains showing Wnt5a expression in the cortical hem (arrowheads) and the postmitotic hippocampal neurons (arrows). **E–E**'' *In situ* hybridization for Wnt5a at E16.5. **F** qPCR showing significant changes in Wnt5a. **G, G**' Photomicrographs of *in situ* Wnt5a in control and *NEX-cre;Foxg1* TG brains at P7. Values are expressed as the mean ± SEM, $n \geq 3$, $^{*}P < 0.05$, $^{**}P < 0.01$. Scale bars, 200 μm.

ventricular zone and the subventricular zone in the *NEX-Cre; Foxg1* cKO mice (Fig. 3A–A') when examined at E14.5. In the controls, apart from the shrinking cortical hem, Wnt5a was also expressed in the postmitotic hippocampal neurons aligned along the medial pallium (Fig. 3B, E). However, in the *NEX-Cre; Foxg1* cKO mice, the expression of Wnt5a was expanded more widely at E14.5 and E16.5 (Fig. 3B', E'). The expression of Wnt3a and Wnt2b was comparable in control and *NEX-Cre; Foxg1* cKO mice (Fig. 3C–D'). Next, *Foxg1* was overexpressed in postmitotic neurons by crossing *NEX-Cre* mice with *CAG-loxp-stop-loxp-Foxg1-IRES-EGFP* mice

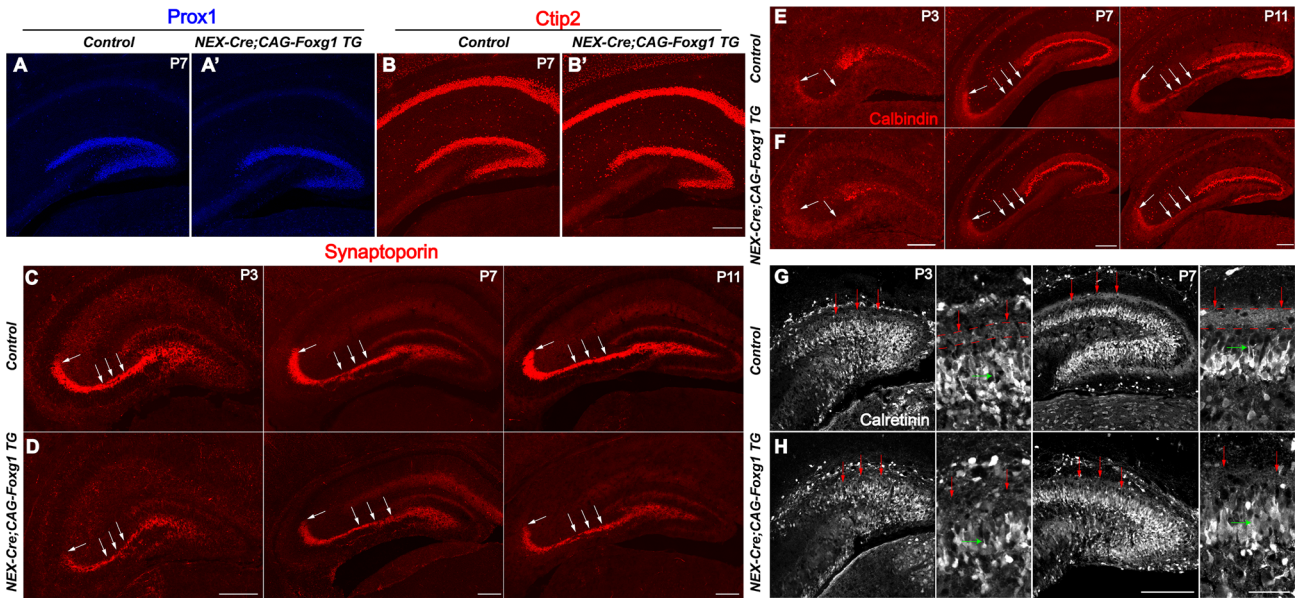

Fig. 4 Impaired development of granule cell dendrites in the *NEX-cre;Foxg1* TG brain. **A–B'** Representative images of P7 mouse brain sections stained with antibodies against Prox1 and Ctip2 to mark granule cells in the DG. **C–F** Immunostaining of anti-Synaptoporin (**C, D**) and Calbindin (**E, F**) showing the mossy fibers (white arrows) at P3, P7, and P11. **G, H** Immunostaining of Calretinin labeling developing dendrites of granule cells at P3 and P7. Red arrows indicate the band formed by the proximal dendrites of granule cells in the molecular layer, while green arrows indicate the dendrites of granule cells. DG, dentate gyrus. Scale bars in magnified views, 50 μm; in **A–H**, 200 μm.

(referred to as *NEX-Cre;CAG- Foxg1* TG) (Fig. 3A''). At the protein level, FOXG1 was strongly increased by ~45% at P0 in the *NEX-Cre; CAG-Foxg1* TG mice (Fig. 3A'''). Downregulation of Wnt5a was evident in the postmitotic neurons in the medial pallium at E14.5 and E16.5, while Wnt3a and Wnt2b were unchanged (Fig. 3B''–E''). qPCR showed a 1.4-fold increase in Wnt5a in the *NEX-Cre;Foxg1* cKO mice and a 0.4-fold decrease in the *NEX-Cre;CAG-Foxg1* TG mice, and that the levels of Wnt3a and Wnt2b were unchanged was also confirmed (Fig. 3F). Wnt5a has been shown to be highly expressed in the DG and CA1 region in postnatal stages (Fig. 3G). Due to postnatal lethality, examination of Wnt5a in the *NEX-Cre; Foxg1*$^{fl/fl}$ cKOs was unachievable. We then assessed Wnt5a in the *NEX-Cre;CAG- Foxg1* TG mice at P7 and found that it was significantly reduced (Fig. 3G'). Taken together, these data indicate that *Foxg1* regulates Wnt5a in postmitotic hippocampal neurons.

Abnormal Development of the Mossy Fibers and Dendrites of Granule Cells in *NEX-Cre; CAG-Foxg1* TG Mice

Wnt5a is involved in axon guidance and outgrowth and was recently shown to be required for dendritic branching [25, 26, 42–44]. Here, we examined the development of mossy fibers and the dendrites of granule cells in the DG of *NEX-Cre;CAG-Foxg1* TG mice. The morphology of the DG was grossly normal at P7, as viewed by immunostaining with anti-Prox1 and Ctip2, specific markers for granule cells (Fig. 4). Next, immunostaining with anti-Synaptoporin and anti-Calbindin were used to examine the mossy fibers at P3, P7, and P11. In controls, long and thick Synaptoporin$^+$ fibers were observed to project to the CA3 region (Fig. 4C). However, in the *NEX-Cre; CAG-Foxg1* TG mice, although mossy fibers properly projected to the CA3 region, they were substantially thinner than those of controls (Fig. 4D). Similar defects were showed by Calbindin immunostaining (Fig. 4E, F). To examine the dendritic development of granule cells, we immunostained with anti-Calretinin at P3 and P7. In the control DGs, Calretinin$^+$ proximal dendrites of granule cells formed a weak band at P3 and a clear band at P7 on the inner side of the molecular layer (Fig. 4G). In the *NEX-Cre;CAG-Foxg1* TG mice, the Calretinin$^+$ band was almost undetectable at P3, and much weaker at P7 than that in controls (Fig. 4H), suggesting a developmental defect in the dendrites of granule cells. To further confirm these defects, we immunostained with anti-Synaptoporin and anti-Calbindin in serial sections of P11 brains. As shown in Figure 5, compared to the control DG, from the rostral to the caudal levels the mossy fibers were thinner in the *NEX-Cre; CAG-Foxg1* TG mice, further demonstrating that Foxg1 is required for the development of mossy fibers.

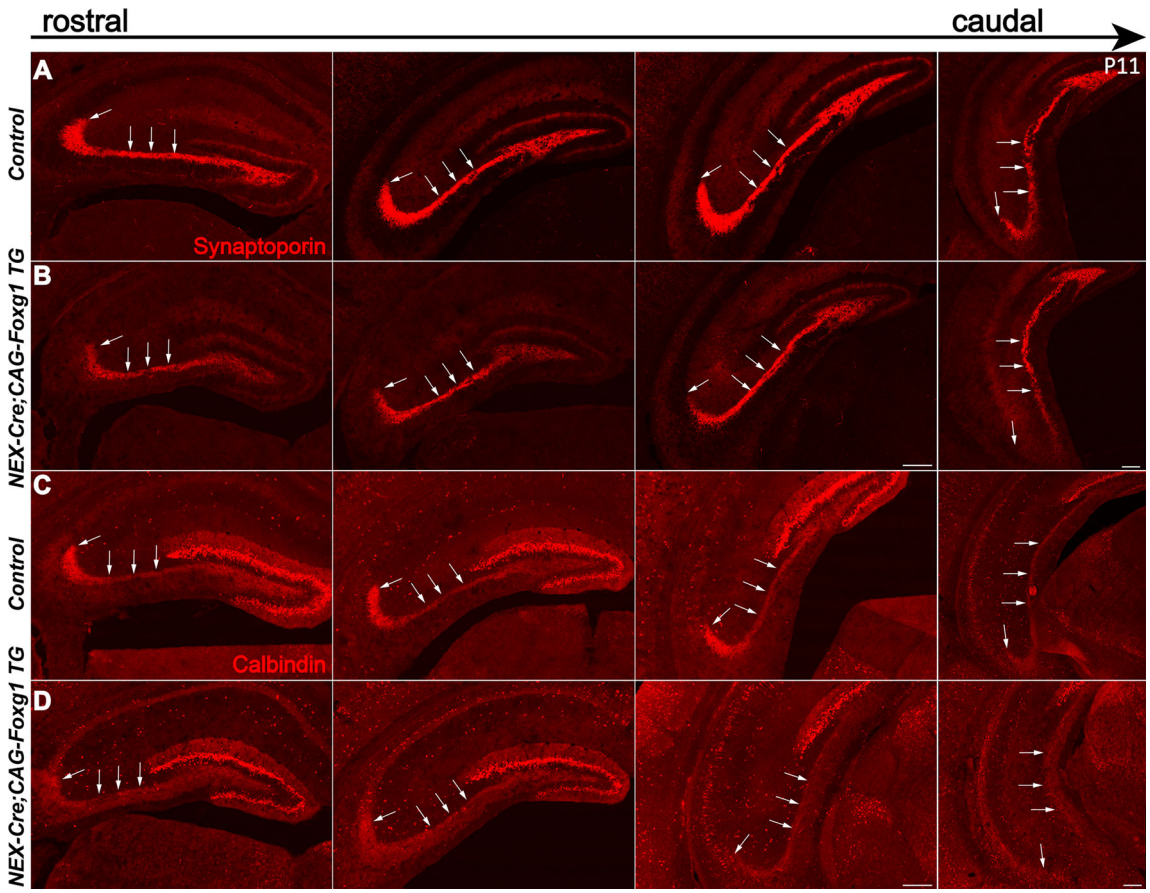

Fig. 5 Impaired development of mossy fibers in the *NEX-cre; Foxg1* TG brain at P11. **A–D** Immunostaining of anti-Synaptoporin (**A, B**) and Calbindin (**C, D**) showing the mossy fibers (white arrows), from the rostral to the caudal levels. Scale bars, 200 μm.

We then used Golgi-Cox staining to further explore the developmental dendritic defects. At P17 in controls, the dendritic tree of granule cells was well developed with numerous and complicated arbors (Fig. 6A). In contrast, we observed a substantial reduction in the dendritic complexity in the *NEX-Cre*;*CAG- Foxg1* TG mice (Fig. 6B), and the total dendritic length was significantly reduced (Fig. 6C). We next quantified the dendritic complexity by counting the intersections where the dendrites crossed the concentric circles drawn at 20-μm intervals around a granule cell body. Statistical analysis showed a strong decrease in the number of intersections compared with the control neurons (Fig. 6D). Similar deficits were observed in CA1 pyramidal neurons (Fig. 6E, F). The total dendritic length was reduced by ~24% (Fig. 6G), and the number of intersections was also significantly decreased in the *NEX-Cre*; *CAG-Foxg1* TG mice (Fig. 6H). Together, these results suggest that the Foxg1-Wnt5a signaling pathway is required for the development of neurites in the DG as well as the CA region.

FOXG1 Directly Represses Wnt5a

To investigate whether FOXG1 directly regulates Wnt5a, we analyzed the *Wnt5a* locus and found three putative FOXG1 consensus binding motifs: one was located at the promotor domain (0.2 kb upstream of the transcription start site, RefSeq accession number: NM_ 009524), and the other two were 6.3 kb and 194.6 kb downstream enhancer sites (Fig. 7A, referred to as Prmt, E1, and E2, respectively). ChIP-qPCR was then carried out, and showed 15.89 ± 2.49-fold, 7.89 ± 0.91-fold, and 10.02 ± 1.32-fold enrichment of FOXG1 on Prmt, E1, and E2, respectively (Fig. 7B). The luciferase assay showed that when PGL3-Prmt was co-transfected with PCAG-*Foxg1*, the activity was reduced by ~36.0 ± 9.4% ($P < 0.05$). No significant inhibition was detected when PGL3-E1 was co-transfected with PCAG-*Foxg1*. The luciferase activity was reduced by ~30.4 ± 6.8% ($P < 0.05$) when PGL3-E2 was co-transfected (Fig. 7C). Thus, Foxg1 directly binds to the promotor and E2 enhancer domains to repress Wnt5a expression.

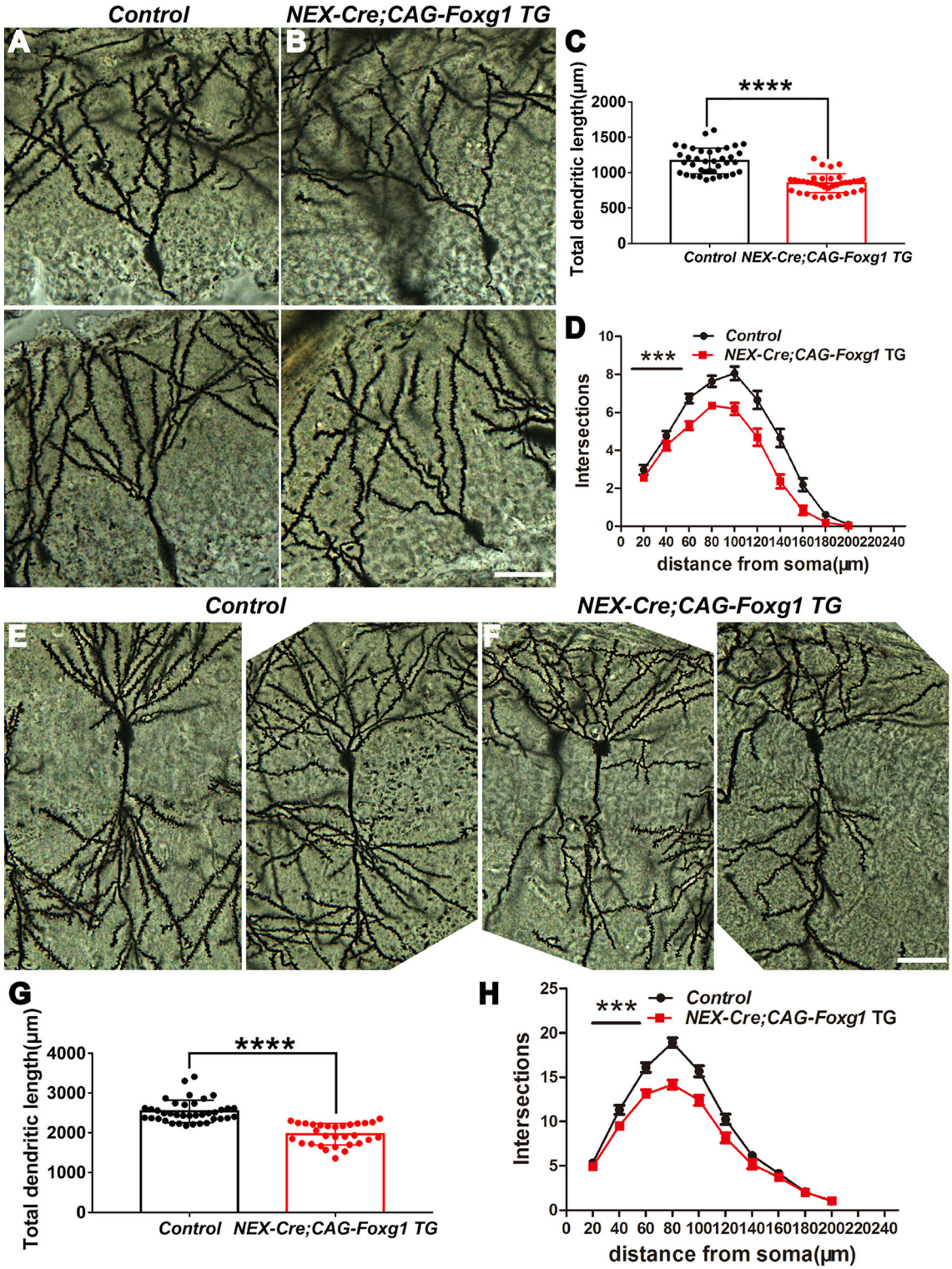

Fig. 6 Reduced dendritic complexity in CA1 and DG after *Foxg1* overexpression. **A, B** Representative images showing the morphology of granule cells at P17 in control and TG mice by Golgi staining. **C** Total dendritic length is significantly reduced in *NEX-cre;Foxg1* TG mice (control, $n = 38$ cells from 5 mice; TG, $n = 36$ cells from 5 mice, $^{****}P < 0.0001$; *t*-test). **D** Sholl analysis of the dendritic complexity of granule cells (control, $n = 38$ cells from 5 mice; TG, $n = 36$ cells from 5 mice, $^{***}P < 0.0001$; two-way ANOVA). **E, F** Representative images of Golgi-stained CA1 pyramidal neurons from control (**E**) and TG (**F**) mice. G Total dendritic length of CA1 pyramidal neurons is also reduced in TG mice (control, $n = 38$ cells from 5 mice; TG, $n = 30$ cells from 5 mice, $^{****}P < 0.0001$; *t*-test). **H** Sholl analysis of the dendritic complexity of hippocampal CA1 pyramidal neurons (control, $n = 38$ cells from 5 mice; TG, $n = 30$ cells from 5 mice; $^{***}P < 0.0001$; two-way ANOVA). CA, cornu ammonis; scale bars, 20 μm.

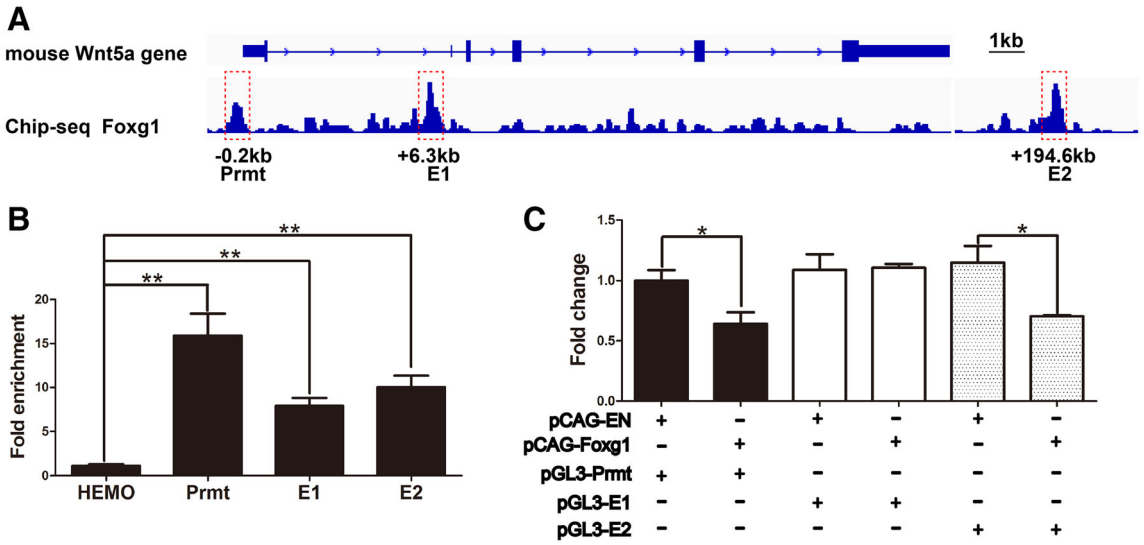

Fig. 7 FOXG1 represses Wnt5a by directly binding its promoter and E2 enhancer sites. **A** Three FOXG1 consensus binding sites denoted Prmt, E1, and E2 at the Wnt5a gene locus. **B** ChIP-QPCR exhibits high enrichment of FOXG1 on the three hypothetical loci (n = 3, $^{**}P < 0.01$). **C** Luciferase assays showing significant inhibition of Wnt5a by FOXG1 through the promoter and E2 sites (n = 4, $^{*}P < 0.05$; Student's t-test).

Discussion

Wnt signaling plays crucial roles in various developmental processes [1, 5, 6, 45–52]. Wnt5a has been demonstrated to be required for axon outgrowth, dendrite morphogenesis, and synaptic plasticity [25, 27, 42, 44, 53, 54]. However, how Wnt5a is regulated remains unclear. In this study, we report that *Foxg1* suppressed Wnt5a directly during the development of the hippocampus at both embryonic and postnatal stages (Fig. 8).

FOXG1 has been shown to interact with Wnt signaling in a complicated way. FOXG1 transcriptionally suppresses Wnt8b during optic development [32]. During early facial and forebrain development, the canonical Wnt/ß-catenin pathway targets Fgf8 signaling, which subsequently triggers *Foxg1* expression [33, 34]. Interestingly, in Wnt3a mutants, *Foxg1* is severely reduced in the truncated medial neuroepithelium [9]. On the other hand, in *Foxg1*-null mutants in which *Foxg1* is disrupted as early as E8.5, the cortical hem markedly expands into the neocortex with the

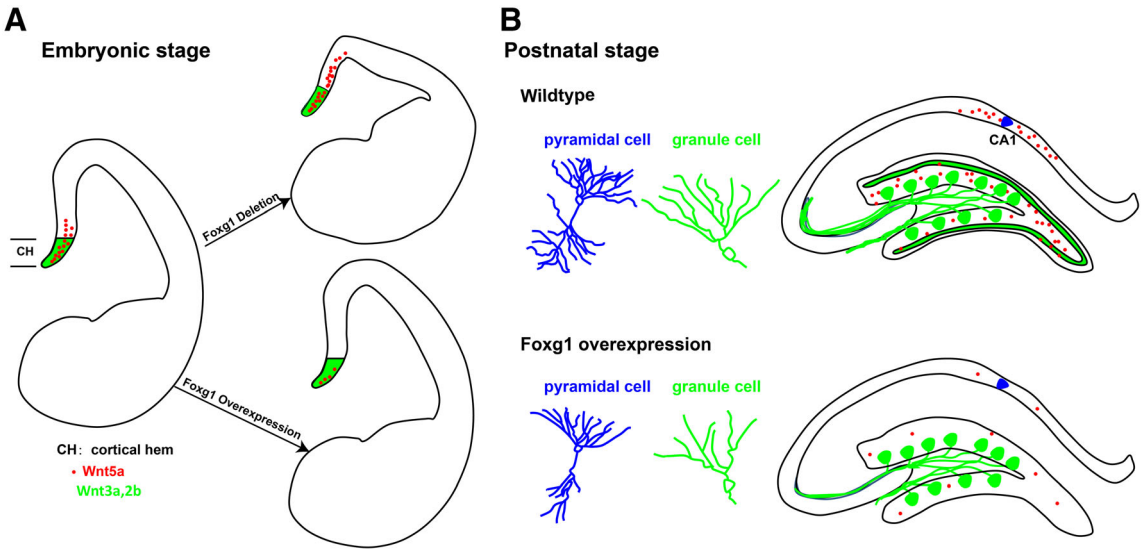

Fig. 8 Schematic representation of the role of *Foxg1* in hippocampal development *via* Wnt5a. **A** During the embryonic stage (E12.5–E14.5), deletion of *Foxg1* leads to expansion of the Wnt5a-expressing region, while *Foxg1*-overexpression represses Wnt5a expression in the hippocampal primordium. **B** During postnatal development, forced expression of *Foxg1* in postmitotic pyramidal and granule cells leads to downregulation of wnt5a and disturbs the development of dendrites and mossy fibers.

expression of Wnt3a, Wnt2b and Wnt5a spread throughout the whole cortical field [31]. Here, we showed that deletion of *Foxg1* from E10.5 onwards did not cause expansion of the cortical hem, while Wnt3a and Wnt2b exhibited a normal expression pattern. Interestingly, we found that Wnt5a was upregulated. Moreover, Wnt5a expression was significantly increased when FOXG1 was deleted in postmitotic neurons in the medial pallium from which the hippocampus and the DG are derived. Overexpression of *Foxg1* reduced Wnt5a but had no effects on Wnt3a/Wnt2b. We further demonstrated that FOXG1 directly suppressed Wnt5a by binding to its promoter and enhancer domains. Our results suggest that FOXG1 regulates Wnt5a but not Wnt3a/Wnt2b in the medial pallium during telencephalic development and expand our knowledge of the interaction between Foxg1 and Wnt signaling.

In mammals, the hippocampus plays a crucial role in learning and memory [55–60]. During mnemonic functions, the hippocampus coordinates the interactions among brain areas including the medial prefrontal cortex, medial entorhinal cortex, and amygdala, to which the CA1 pyramidal neurons project [61–64]. The DG receives information from the entorhinal cortex and serves as the primary afferent pathway into the hippocampus [65–67]. Dysfunction of the neural circuits is closely associated with a variety of neurological disorders [68–71]. Patients suffering from FOXG1 syndrome have severe cognitive defects [72–75]. Duplications of FOXG1 are associated with cognitive defects and mental retardation [76–78]. Studies using mouse models have shown that *Foxg1* is involved in hippocampal formation as well as neurite development [35, 40]. Recently, Wnt5a was reported to be required for dendrite branching and growth in hippocampal neurons [21]. Wnt5a also regulates axon guidance and outgrowth [25, 26, 44, 79]. In the present study, loss of *Foxg1* led to evident upregulation of Wnt5a in the hippocampal primordium, while overexpression of *Foxg1* resulted in dramatic downregulation of Wnt5a in the granule cells and pyramidal neurons, accompanied by reduced dendritic complexity and mossy fibers. Our study showed that FOXG1 acts as a direct repressor of Wnt5a. FOXG1 suppresses Wnt5a not only at early developmental stages but also in postnatal hippocampal development. Our results help to elucidate the mechanisms underlying the interaction between Foxg1 and Wnt signaling during telencephalic development.

Acknowledgements We thank Yiquan Wei and Li Liu for their assistance in the laboratory and with animal care, and other members of the laboratory for helpful discussions. This work was supported by grants from the National Natural Science Foundation of China (31930045 and 81870899) and the National Key R&D Program of China (2016YFA0501001).

Conflict of interest The authors have no conflicts of interest to declare.

References

1. Ikeya M, Lee SM, Johnson JE, McMahon AP, Takada S. Wnt signalling required for expansion of neural crest and CNS progenitors. Nature 1997, 389: 966–970.
2. Dorsky RI, Moon RT, Raible DW. Control of neural crest cell fate by the Wnt signalling pathway. Nature 1998, 396: 370–373.
3. Kiecker C, Niehrs C. A morphogen gradient of Wnt/beta-catenin signalling regulates anteroposterior neural patterning in Xenopus. Development 2001, 128: 4189–4201.
4. Houart C, Caneparo L, Heisenberg C, Barth K, Take-Uchi M, Wilson S. Establishment of the telencephalon during gastrulation by local antagonism of Wnt signaling. Neuron 2002, 35: 255–265.
5. Lyuksyutova AI, Lu CC, Milanesio N, King LA, Guo N, Wang Y, *et al.* Anterior-posterior guidance of commissural axons by Wnt-frizzled signaling. Science 2003, 302: 1984–1988.
6. Rosso SB, Sussman D, Wynshaw-Boris A, Salinas PC. Wnt signaling through Dishevelled, Rac and JNK regulates dendritic development. Nat Neurosci 2005, 8: 34–42.
7. Vallee A, Lecarpentier Y, Guillevin R, Vallee JN. Opposite interplay between the canonical WNT/beta-catenin pathway and PPAR gamma: A potential therapeutic target in gliomas. Neurosci Bull 2018, 34: 573–588.
8. Takada S, Stark KL, Shea MJ, Vassileva G, McMahon JA, McMahon AP. Wnt-3a regulates somite and tailbud formation in the mouse embryo. Genes Dev 1994, 8: 174–189.
9. Lee SM, Tole S, Grove E, McMahon AP. A local Wnt-3a signal is required for development of the mammalian hippocampus. Development 2000, 127: 457–467.
10. Shruster A, Offen D. Targeting neurogenesis ameliorates danger assessment in a mouse model of Alzheimer's disease. Behav Brain Res 2014, 261: 193–201.
11. Xu N, Zhou WJ, Wang Y, Huang SH, Li X, Chen ZY. Hippocampal Wnt3a is necessary and sufficient for contextual fear memory acquisition and consolidation. Cereb Cortex 2015, 25: 4062–4075.
12. Stanganello E, Zahavi EE, Burute M, Smits J, Jordens I, Maurice MM, *et al.* Wnt signaling directs neuronal polarity and axonal growth. iScience 2019, 13: 318–327.
13. Katoh M. WNT2B: comparative integromics and clinical applications (Review). Int J Mol Med 2005, 16: 1103–1108.
14. Katoh M, Kirikoshi H, Terasaki H, Shiokawa K. WNT2B2 mRNA, up-regulated in primary gastric cancer, is a positive regulator of the WNT- beta-catenin-TCF signaling pathway. Biochem Biophys Res Commun 2001, 289: 1093–1098.
15. Kubo F, Takeichi M, Nakagawa S. Wnt2b inhibits differentiation of retinal progenitor cells in the absence of Notch activity by downregulating the expression of proneural genes. Development 2005, 132: 2759–2770.
16. Cho SH, Cepko CL. Wnt2b/beta-catenin-mediated canonical Wnt signaling determines the peripheral fates of the chick eye. Development 2006, 133: 3167–3177.
17. Ciani L, Salinas PC. WNTs in the vertebrate nervous system: from patterning to neuronal connectivity. Nat Rev Neurosci 2005, 6: 351–362.
18. Yoshikawa S, McKinnon RD, Kokel M, Thomas JB. Wnt-mediated axon guidance *via* the *Drosophila* Derailed receptor. Nature 2003, 422: 583–588.
19. Logan CY, Nusse R. The Wnt signaling pathway in development and disease. Annu Rev Cell Dev Biol 2004, 20: 781–810.

20. Grove EA, Tole S, Limon J, Yip L, Ragsdale CW. The hem of the embryonic cerebral cortex is defined by the expression of multiple Wnt genes and is compromised in Gli3-deficient mice. Development 1998, 125: 2315–2325.
21. Chen CM, Orefice LL, Chiu SL, LeGates TA, Hattar S, Huganir RL*, et al.* Wnt5a is essential for hippocampal dendritic maintenance and spatial learning and memory in adult mice. Proc Natl Acad Sci U S A 2017, 114: E619–E628.
22. Zhang X, Zhu J, Yang GY, Wang QJ, Qian L, Chen YM*, et al.* Dishevelled promotes axon differentiation by regulating atypical protein kinase C. Nat Cell Biol 2007, 9: 743–754.
23. Shafer B, Onishi K, Lo C, Colakoglu G, Zou Y. Vangl2 promotes Wnt/planar cell polarity-like signaling by antagonizing Dvl1-mediated feedback inhibition in growth cone guidance. Dev Cell 2011, 20: 177–191.
24. Zou Y, Lyuksyutova AI. Morphogens as conserved axon guidance cues. Curr Opin Neurobiol 2007, 17: 22–28.
25. Li L, Hutchins BI, Kalil K. Wnt5a induces simultaneous cortical axon outgrowth and repulsive axon guidance through distinct signaling mechanisms. J Neurosci 2009, 29: 5873–5883.
26. Blakely BD, Bye CR, Fernando CV, Horne MK, Macheda ML, Stacker SA*, et al.* Wnt5a regulates midbrain dopaminergic axon growth and guidance. PLoS One 2011, 6: e18373.
27. Bian WJ, Miao WY, He SJ, Wan ZF, Luo ZG, Yu X. A novel Wnt5a-Frizzled4 signaling pathway mediates activity-independent dendrite morphogenesis via the distal PDZ motif of Frizzled 4. Dev Neurobiol 2015, 75: 805–822.
28. Godbole G, Shetty AS, Roy A, D'Souza L, Chen B, Miyoshi G*, et al.* Hierarchical genetic interactions between FOXG1 and LHX2 regulate the formation of the cortical hem in the developing telencephalon. Development 2018, 145.
29. Du A, Wu X, Chen H, Bai QR, Han X, Liu B*, et al.* Foxg1 directly represses Dbx1 to confine the POA and subsequently regulate ventral telencephalic patterning. Cereb Cortex 2019, 29: 4968–4981.
30. Hanashima C, Li SC, Shen L, Lai E, Fishell G. Foxg1 suppresses early cortical cell fate. Science 2004, 303: 56–59.
31. Muzio L, Mallamaci A. Foxg1 confines Cajal-Retzius neuronogenesis and hippocampal morphogenesis to the dorsomedial pallium. J Neurosci 2005, 25: 4435–4441.
32. Smith R, Huang YT, Tian T, Vojtasova D, Mesalles-Naranjo O, Pollard SM*, et al.* The transcription factor Foxg1 promotes optic fissure closure in the mouse by suppressing Wnt8b in the nasal optic stalk. J Neurosci 2017, 37: 7975–7993.
33. Shimamura K, Rubenstein JL. Inductive interactions direct early regionalization of the mouse forebrain. Development 1997, 124: 2709–2718.
34. Wang Y, Song L, Zhou CJ. The canonical Wnt/beta-catenin signaling pathway regulates Fgf signaling for early facial development. Dev Biol 2011, 349: 250–260.
35. Tian C, Gong Y, Yang Y, Shen W, Wang K, Liu J*, et al.* Foxg1 has an essential role in postnatal development of the dentate gyrus. J Neurosci 2012, 32: 2931–2949.
36. Liu B, Xiao H, Zhao C. Forced expression of Foxg1 in the cortical hem leads to the transformation of cajal-retzius cells into dentate granule neurons. J Dev Biol 2018, 6.
37. Goebbels S, Bormuth I, Bode U, Hermanson O, Schwab MH, Nave KA. Genetic targeting of principal neurons in neocortex and hippocampus of NEX-Cre mice. Genesis 2006, 44: 611–621.
38. Wu X, Gu X, Han X, Du A, Jiang Y, Zhang X*, et al.* A novel function for Foxm1 in interkinetic nuclear migration in the developing telencephalon and anxiety-related behavior. J Neurosci 2014, 34: 1510–1522.
39. Su Y, Liu J, Yu B, Ba R, Zhao C. Brpf1 haploinsufficiency impairs dendritic arborization and spine formation, leading to cognitive deficits. Front Cell Neurosci 2019, 13: 249.
40. Yu B, Liu J, Su M, Wang C, Chen H, Zhao C. Disruption of Foxg1 impairs neural plasticity leading to social and cognitive behavioral defects. Mol Brain 2019, 12: 63.
41. Han X, Gu X, Zhang Q, Wang Q, Cheng Y, Pleasure SJ*, et al.* FoxG1 directly represses dentate granule cell fate during forebrain development. Front Cell Neurosci 2018, 12: 452.
42. Keeble TR, Halford MM, Seaman C, Kee N, Macheda M, Anderson RB*, et al.* The Wnt receptor Ryk is required for Wnt5a-mediated axon guidance on the contralateral side of the corpus callosum. J Neurosci 2006, 26: 5840–5848.
43. Blakely BD, Bye CR, Fernando CV, Prasad AA, Pasterkamp RJ, Macheda ML*, et al.* Ryk, a receptor regulating Wnt5a-mediated neurogenesis and axon morphogenesis of ventral midbrain dopaminergic neurons. Stem Cells Dev 2013, 22: 2132–2144.
44. Clark CE, Richards LJ, Stacker SA, Cooper HM. Wnt5a induces Ryk-dependent and -independent effects on callosal axon and dendrite growth. Growth Factors 2014, 32: 11–17.
45. Davis EK, Zou Y, Ghosh A. Wnts acting through canonical and noncanonical signaling pathways exert opposite effects on hippocampal synapse formation. Neural Dev 2008, 3: 32.
46. Theil T, Aydin S, Koch S, Grotewold L, Ruther U. Wnt and Bmp signalling cooperatively regulate graded Emx2 expression in the dorsal telencephalon. Development 2002, 129: 3045–3054.
47. Nordin N, Li M, Mason JO. Expression profiles of Wnt genes during neural differentiation of mouse embryonic stem cells. Cloning Stem Cells 2008, 10: 37–48.
48. Fotaki V, Larralde O, Zeng S, McLaughlin D, Nichols J, Price DJ*, et al.* Loss of Wnt8b has no overt effect on hippocampus development but leads to altered Wnt gene expression levels in dorsomedial telencephalon. Dev Dyn 2010, 239: 284–296.
49. Fotaki V, Price DJ, Mason JO. Wnt/beta-catenin signaling is disrupted in the extra-toes (Gli3(Xt/Xt)) mutant from early stages of forebrain development, concomitant with anterior neural plate patterning defects. J Comp Neurol 2011, 519: 1640–1657.
50. Harrison-Uy SJ, Pleasure SJ. Wnt signaling and forebrain development. Cold Spring Harb Perspect Biol 2012, 4: a008094.
51. Shimogori T, Banuchi V, Ng HY, Strauss JB, Grove EA. Embryonic signaling centers expressing BMP, WNT and FGF proteins interact to pattern the cerebral cortex. Development 2004, 131: 5639–5647.
52. Cuesta S, Funes A, Pacchioni AM. Social isolation in male rats during adolescence inhibits the Wnt/beta-catenin pathway in the prefrontal cortex and enhances anxiety and cocaine-induced plasticity in adulthood. Neurosci Bull 2020, 36: 611–624.
53. Farias GG, Alfaro IE, Cerpa W, Grabowski CP, Godoy JA, Bonansco C*, et al.* Wnt-5a/JNK signaling promotes the clustering of PSD-95 in hippocampal neurons. J Biol Chem 2009, 284: 15857–15866.
54. Varela-Nallar L, Alfaro IE, Serrano FG, Parodi J, Inestrosa NC. Wingless-type family member 5A (Wnt-5a) stimulates synaptic differentiation and function of glutamatergic synapses. Proc Natl Acad Sci U S A 2010, 107: 21164–21169.
55. Eichenbaum H. Hippocampus: cognitive processes and neural representations that underlie declarative memory. Neuron 2004, 44: 109–120.
56. Lisman JE, Grace AA. The hippocampal-VTA loop: controlling the entry of information into long-term memory. Neuron 2005, 46: 703–713.
57. Aimone JB, Wiles J, Gage FH. Potential role for adult neurogenesis in the encoding of time in new memories. Nat Neurosci 2006, 9: 723–727.
58. Surget A, Tanti A, Leonardo ED, Laugeray A, Rainer Q, Touma C*, et al.* Antidepressants recruit new neurons to improve stress response regulation. Mol Psychiatry 2011, 16: 1177–1188.

59. Zhang L, Luo XP. Plasticity and metaplasticity of lateral perforant path in hippocampal dentate gyrus in a rat model of febrile seizure. Acta Physiol Sin 2011, 63: 124–130.
60. Ji C, Zhu L, Chen C, Wang S, Zheng L, Li H. Volumetric changes in hippocampal subregions and memory performance in mesial temporal lobe epilepsy with hippocampal sclerosis. Neurosci Bull 2018, 34: 389–396.
61. Cenquizca LA, Swanson LW. Spatial organization of direct hippocampal field CA1 axonal projections to the rest of the cerebral cortex. Brain Res Rev 2007, 56: 1–26.
62. Maren S, Quirk GJ. Neuronal signalling of fear memory. Nat Rev Neurosci 2004, 5: 844–852.
63. Fanselow MS, Poulos AM. The neuroscience of mammalian associative learning. Annu Rev Psychol 2005, 56: 207–234.
64. Lee SH, Marchionni I, Bezaire M, Varga C, Danielson N, Lovett-Barron M, *et al.* Parvalbumin-positive basket cells differentiate among hippocampal pyramidal cells. Neuron 2014, 82: 1129–1144.
65. Blackstad TW. Commissural connections of the hippocampal region in the rat, with special reference to their mode of termination. J Comp Neurol 1956, 105: 417–537.
66. Blackstad TW. On the termination of some afferents to the hippocampus and fascia dentata; an experimental study in the rat. Acta Anat (Basel) 1958, 35: 202–214.
67. Forster E, Zhao S, Frotscher M. Laminating the hippocampus. Nat Rev Neurosci 2006, 7: 259–267.
68. Yizhar O, Fenno LE, Prigge M, Schneider F, Davidson TJ, O'Shea DJ, *et al.* Neocortical excitation/inhibition balance in information processing and social dysfunction. Nature 2011, 477: 171–178.
69. Paluszkiewicz SM, Martin BS, Huntsman MM. Fragile X syndrome: the GABAergic system and circuit dysfunction. Dev Neurosci 2011, 33: 349–364.
70. Xu W, Sudhof TC. A neural circuit for memory specificity and generalization. Science 2013, 339: 1290–1295.
71. Ferhat AT, Halbedl S, Schmeisser MJ, Kas MJ, Bourgeron T, Ey E. Behavioural phenotypes and neural circuit dysfunctions in mouse models of autism spectrum disorder. Adv Anat Embryol Cell Biol 2017, 224: 85–101.
72. Kortum F, Das S, Flindt M, Morris-Rosendahl DJ, Stefanova I, Goldstein A, *et al.* The core FOXG1 syndrome phenotype consists of postnatal microcephaly, severe mental retardation, absent language, dyskinesia, and corpus callosum hypogenesis. J Med Genet 2011, 48: 396–406.
73. Pratt DW, Warner JV, Williams MG. Genotyping FOXG1 mutations in patients with clinical evidence of the FOXG1 syndrome. Mol Syndromol 2013, 3: 284–287.
74. Shoichet SA, Kunde SA, Viertel P, Schell-Apacik C, von Voss H, Tommerup N, *et al.* Haploinsufficiency of novel FOXG1B variants in a patient with severe mental retardation, brain malformations and microcephaly. Hum Genet 2005, 117: 536–544.
75. Le Guen T, Bahi-Buisson N, Nectoux J, Boddaert N, Fichou Y, Diebold B, *et al.* A FOXG1 mutation in a boy with congenital variant of Rett syndrome. Neurogenetics 2011, 12: 1–8.
76. Brunetti-Pierri N, Paciorkowski AR, Ciccone R, Della Mina E, Bonaglia MC, Borgatti R, *et al.* Duplications of FOXG1 in 14q12 are associated with developmental epilepsy, mental retardation, and severe speech impairment. Eur J Hum Genet 2011, 19: 102–107.
77. Yeung A, Bruno D, Scheffer IE, Carranza D, Burgess T, Slater HR, *et al.* 4.45 Mb microduplication in chromosome band 14q12 including FOXG1 in a girl with refractory epilepsy and intellectual impairment. Eur J Med Genet 2009, 52: 440–442.
78. Tohyama J, Yamamoto T, Hosoki K, Nagasaki K, Akasaka N, Ohashi T, *et al.* West syndrome associated with mosaic duplication of FOXG1 in a patient with maternal uniparental disomy of chromosome 14. Am J Med Genet A 2011, 155A: 2584–2588.
79. Coullery RP, Ferrari ME, Rosso SB. Neuronal development and axon growth are altered by glyphosate through a WNT non-canonical signaling pathway. Neurotoxicology 2016, 52: 150–161.